



UNIVERSITY OF LEEDS

This is a repository copy of *Microstructure and long-term stability of spray dried emulsions with ultra-high oil content*.

White Rose Research Online URL for this paper:  
<http://eprints.whiterose.ac.uk/89585/>

Version: Accepted Version

---

**Article:**

Sarkar, A, Arfsten, J, Golay, PA et al. (2 more authors) (2016) Microstructure and long-term stability of spray dried emulsions with ultra-high oil content. *Food Hydrocolloids*, 52. 857 - 867. ISSN 0268-005X

<https://doi.org/10.1016/j.foodhyd.2015.09.003>

---

© 2015, Elsevier. Licensed under the Creative Commons Attribution-NonCommercial-NoDerivatives 4.0 International  
<http://creativecommons.org/licenses/by-nc-nd/4.0/>

**Reuse**

Unless indicated otherwise, fulltext items are protected by copyright with all rights reserved. The copyright exception in section 29 of the Copyright, Designs and Patents Act 1988 allows the making of a single copy solely for the purpose of non-commercial research or private study within the limits of fair dealing. The publisher or other rights-holder may allow further reproduction and re-use of this version - refer to the White Rose Research Online record for this item. Where records identify the publisher as the copyright holder, users can verify any specific terms of use on the publisher's website.

**Takedown**

If you consider content in White Rose Research Online to be in breach of UK law, please notify us by emailing [eprints@whiterose.ac.uk](mailto:eprints@whiterose.ac.uk) including the URL of the record and the reason for the withdrawal request.



[eprints@whiterose.ac.uk](mailto:eprints@whiterose.ac.uk)  
<https://eprints.whiterose.ac.uk/>

1 **Microstructure and long-term stability of spray dried**  
2 **emulsions with ultra-high oil content**

3  
4  
5 **Anwasha Sarkar<sup>1,2\*</sup>, Judith Arfsten<sup>2</sup>, Pierre-Alain Golay<sup>2</sup>, Simone**  
6 **Acquistapace<sup>2</sup> and Emmanuel Heinrich<sup>2</sup>**

7  
8 <sup>1</sup> Food Colloids and Processing Group, School of Food Science and Nutrition,  
9 University of Leeds, Leeds LS2 9JT, UK

10 <sup>2</sup> Nestlé Research Center, Vers-chez-les-Blanc, P.O. Box 44, CH-1000 Lausanne 26,  
11 Switzerland

12  
13 \*Corresponding author:

14 Dr. Anwasha Sarkar

15 Food Colloids and Processing Group,

16 School of Food Science and Nutrition, University of Leeds, Leeds LS2 9JT, UK.

17 E-mail address: [A.Sarkar@leeds.ac.uk](mailto:A.Sarkar@leeds.ac.uk) (A. Sarkar).

18 Tel.: +44 (0) 113 3432748.

## 25 **Abstract**

26 The aim of this study was to investigate the microstructure and long-term mechanical  
27 as well oxidative stability of a new class of spray dried emulsion containing ultrahigh  
28 oil content. Emulsion (20 wt% oil) stabilized by whey protein (1 wt%) was thermally  
29 cross-linked at 82°C for 10 minutes and spray dried without any additional wall  
30 materials using inlet/ outlet air temperature of  $105 \pm 2 / 65 \pm 2$  °C, respectively at a  
31 pilot scale. Confocal micrograph showed cohesive cross-linked whey protein film  
32 present at the oil-water interface and at the powder surface stabilising the oil powder  
33 particles containing 95.3 wt% oil. The mean droplet size of parent emulsion (0.21,  
34 0.38, 0.76, 2.31  $\mu\text{m}$ ) significantly influenced the mechanical stability of the resulting  
35 oil powder in terms of oil leakage (2.73, 0.93, 4.1, 7.54 wt%) upon compaction.  
36 Scanning electron microscopy revealed the level of surface oil and porous “sponge”  
37 like internal microstructure of the oil powder with polyhedral, closely packed  
38 droplets. Strong correlations existed between the mechanical properties of the oil  
39 powder and the oxidative stability over 5 months. The kinetics of oxidation of oil  
40 powder was higher than that of corresponding bulk oil with or without added  
41 antioxidants as evidenced by evolution of primary oxidation products  
42 (hydroperoxides) and secondary oxidation products (hexanal). This might be due to  
43 the multi-step processing (e.g. homogenization, thermal cross-linking, spray drying)  
44 as well as inability of the cohesive but permeable protein matrix to protect the ultra-  
45 high content of oil droplets from diffusion of oxygen and prooxidants.

46

## 47 **Keywords**

48 Spray dried emulsion, oil powder, ultra-high oil content, mechanical stability, oil  
49 oxidation, cross-linked interface

## 50 **1 Introduction**

51 The use of solid-like hydrophobic matrices such as high internal phase emulsion gels  
52 with tuneable properties have been known for applications in fuels, oil recovery,  
53 pharmaceutical and personal care industries (Cameron, 2005). Recently, there has  
54 been increasing research interests of creating such high internal phase hydrophobic  
55 matrices using food grade ingredients to alter rheological properties as well as to  
56 impart solid-fat functionality to liquid oils using environment friendly ingredients and  
57 processing conditions (Nikiforidis & Scholten, 2015; Patel, Rodriguez, Lesaffer, &  
58 Dewettinck, 2014; Romoscanu & Mezzenga, 2006). An alternative approach to create  
59 structured hydrophobic liquids is to create oil powder using emulsion templating as a  
60 starting point followed by spray drying where the resulting oil powder will contain  
61 ultrahigh content.

62 Spray drying is one of the oldest and most widely used encapsulation methods  
63 in food industries to deliver emulsified food ingredients such as flavours and other  
64 lipophilic bioactive ingredients (Ixtaina, Julio, Wagner, Nolasco, & Tomás, 2015;  
65 Jafari, Assadpoor, Bhandari, & He, 2008; Taneja, Ye, Jones, Archer, & Singh, 2013).  
66 The process of creation of spray dried systems based on oil-in-water emulsion  
67 involves creation of emulsions using homogenization, followed by addition of wall  
68 material (e.g. starch, lactose, maltodextrin, polysaccharides) before atomization of the  
69 mixture into the drying chamber. The addition of carbohydrate based wall materials  
70 enables formation of glassy matrices to retard the diffusion of oxygen and enhance  
71 oxidative stability (Ubbink & Krüger, 2006). However, the compromise lies in the oil  
72 content in resulting powder being 5-30 wt%.

73 A promising new route to create oil powder with 90 wt% oil content from  
74 liquid oil has been developed by Mezzenga & Ulrich (2010). The method has utilized

75 protein-stabilized oil-water interface ( $\beta$ -lactoglobulin), cross-linking the protein  
76 absorbed at the interfaces via a heat denaturation process and successively spray  
77 drying without the addition of any carbohydrates. Thus, this approach resulted in  
78 decreasing the solid dry base and enhancing the content of hydrophobic liquid of the  
79 final powder. Thermal cross-linking of the interfacial layer after emulsion provided  
80 enough elasticity to the interfaces and sufficient barrier against droplet coalescence. A  
81 key open question lies in the oxidative stability of such oil powders with ultra-high oil  
82 content. In addition, a critical issue often faced when dealing with encapsulated oil  
83 systems is that the oil might leak out during processing food applications in industrial  
84 line or bulk compression during shipping over distances due to the insufficient  
85 mechanical strength of the matrices to survive shear and normal stresses.

86 Hence, the objective of this study was to first understand the microstructure  
87 and morphology of spray dried emulsions with ultra-high oil levels at a molecular  
88 level and then to investigate the long-term mechanical stability and oxidative stability  
89 of such new class of microstructure over a period of 5 months. In this study, spray  
90 dried whey protein-stabilized emulsion with resulting powder containing ultra-high  
91 oil levels (> 95 wt%) was created using appropriate formulation design and a scaled  
92 up approach. Post emulsion creation, heat treatment of 82 °C/ 10 minutes was used to  
93 enable whey protein denaturation followed by irreversible aggregation reactions at the  
94 oil-water interface involving hydrogen bonding, hydrophobic interactions and  
95 covalent disulphide linkages resulting in formation of cross-linked film (Euston,  
96 Finnigan, & Hirst, 2000; Jiménez-Flores, Ye, & Singh, 2005; Tolkach & Kulozik,  
97 2007; Hammann, & Schmid, 2014) before spray drying. Our hypothesis is that this  
98 cross-linked protein film alone without added carbohydrate molecules enables  
99 emulsions to dry effectively in a spray dryer without oiling off as well as might

100 protect the oil against any mechanical instability and oxidation during long-term  
101 storage.

102 For studying mechanical stability, we have developed a simple and effective  
103 technique to measure quantitatively oil leakage from oil powder under compression  
104 (Bahtz, 2010), which might find its use in food industries. The oxidative stability of  
105 the oil powders was estimated using characterization of a combination of primary  
106 oxidation (hydroperoxides) and secondary oxidation (hexanal) products (Sarkar,  
107 Golay, Acquistapace, & Craft, 2015) with or without the addition of relevant  
108 antioxidants such as ascorbyl palmitate (AP) and mixed tocopherols (M-TOC)  
109 (Velasco, Dobarganes, & Márquez-Ruiz, 2000).

110 To our knowledge, this is the first study that investigates long-term  
111 mechanical and oxidative stability of this new class of spray dried emulsions  
112 containing ultra-high oil levels in a pilot scale.

113

## 114 **2 Materials and Methods**

### 115 2.1 Materials

116 Whey protein isolate (WPI) containing ~ 98% protein (Bipro, Davisco Foods  
117 International, US) was used without any further purification. Refined bleached  
118 deodorized soy oil (SO) was sourced commercially from the Cargill Inc., Brazil.  
119 Upon receipt, oils were stored in their original container in the dark at 4 °C until  
120 evaluated for fatty acid (FA) composition and stability. For the oxidative stability  
121 study, antioxidants such as ascorbyl palmitate (AP) and mixed tocopherols (M-TOC)  
122 purchased from Sigma-Aldrich, US were added to the oils. The M-TOC was a  
123 mixture of  $\alpha$ -,  $\beta$ -,  $\gamma$ - and  $\delta$ -tocopherols and contained  $\geq 500$  mg/g total tocopherol  
124 content as stated by the manufacturer. Chloroform, methanol, hexane, acetic acid and

125 isooctane were purchased from Merck, Darmstadt, Germany. Hexanal, purity 98%  
126 and hexanal-d<sub>12</sub>, isotopic enrichment min. 98% atom were purchased from CDN  
127 Isotopes, Canada. All the solutions were prepared from analytical grade chemicals  
128 unless otherwise specified. Demineralized softened water was used for the preparation  
129 of all solutions.

130

## 131 2.2 Preparation of oil powder with ultra-high oil content

132 Oil powder with ultra-high oil level was prepared at pilot plant level at Nestlé  
133 Research Center, Lausanne using an adapted formulation design based on approach  
134 described by Mezzenga & Ulrich (2010), which is schematically illustrated in Figure  
135 1 and described below.

136

### 137 2.2.1 Emulsion preparation and thermal treatment

138 Protein solution (1.0 wt%) was prepared by dispersing 0.48 kg WPI in 47.52 kg  
139 demineralized softened water (160 mg/ L Na, < 0.1 mg/ 100g Fe, < 0.02 mg/ 100g Cu  
140 and < 0.1 mg/ 100g Zn) water. Protein solution was stirred for 1 h at 20 °C using a  
141 mixer (X50/10, Ystral GmbH, Ballrechten-Dottingen, Germany) to ensure complete  
142 dissolution and adjusted to pH 7 using 0.1 M NaOH/ HCl. 20 wt% oil-in-water  
143 emulsions were prepared by mixing 12 kg soy oil and 48 kg aqueous protein solution.

144 Soy oil was used directly for preparation of emulsions used in this study.  
145 However, for the oxidative stability study, antioxidants (300 ppm AP, 300 ppm AP +  
146 1000 ppm M-TOC) were added with gentle stirring to the SO before emulsion  
147 preparation based on a previous study (Sarkar, et al., 2015). For the pre-  
148 emulsification, oil was slowly added into the aqueous solution over a period of 4 min  
149 and sheared using conventional rotor–stator type mixer (Polytron PT 120/4 M,

150 Kinematica AG, Lucerne, Switzerland) at a speed of 3000 rpm for 10 minutes, until a  
151 target droplet size of 13-15  $\mu\text{m}$  was reached. The pre-emulsions were then  
152 homogenized using a two-stage valve homogenizer (Panda Plus 2000, GEA Niro  
153 Soavi - Homogeneizador Parma, Italy) in continuous mode operating at first stage/  
154 second stage pressures: 2 passes  $\times$  100 / 25, 1 pass  $\times$  200 / 100, 1 pass  $\times$  400 / 100  
155 and 1 pass  $\times$  1200 / 100, to create different droplet sizes as shown in Table 1,  
156 respectively. For the long-term stability study and microstructural characterization,  
157 emulsions created with 1  $\times$  400/ 100 bar pressures were used to prepare the oil  
158 powders.

159 Plate heat exchanger (Alfa Laval, Lund, Sweden) in line with tubular heat  
160 exchanger (Sulzer SMXL DN20, Winterthur, Switzerland) was used for the  
161 subsequent thermal cross-linking of the whey proteins at the oil-water droplet  
162 interfaces. The temperature was increased to 82°C and held for 10 min using tubular  
163 heat exchanger. The cross-linked emulsions were stored at 4°C until its further use.  
164 Emulsions were prepared in triplicates for analyses.

165

### 166 2.3 Spray drying

167 Spray drying of the thermally cross-linked emulsions was performed in a pilot plant  
168 scale spray dryer (Niro SD-6.3-N, GEA Process Engineering A/S, Søborg, Denmark).  
169 The emulsions were fed into the spray tower through a peristaltic pump at a feed flow  
170 rate of 10 L/h and atomized by a spraying rotary disc (25,000 rpm). Inlet and outlet air  
171 temperature were  $105 \pm 2$  and  $65 \pm 2$  °C, respectively. The oil powder was collected  
172 into aluminium pouches and stored at 4 °C unless otherwise mentioned.

173

### 174 2.4 Chemical composition and physical properties

175 Moisture (AOAC 925.04) and crude protein content (AOAC 981.10) of the oil  
176 powder were determined by standard method (AOAC, 1995). The oil content was  
177 measured using adapted Folch extraction method (Dionisi, Golay, Aeschlimann, &  
178 Fay, 1998). Briefly, oil powder was treated with methanol/chloroform mixture (2:1,  
179 v/v) in dark followed by homogenizing using ultraturrax for 2 min to break the  
180 encapsulating protein matrix and then centrifuged at 3000 rpm for 20 min. The liquid  
181 phase was filtered and collected. The sample left in the centrifuge tube was  
182 homogenized for 2 min with chloroform / methanol (1:1, v/v). After the second  
183 centrifugation, the liquid phase was filtered and added to the previous collection. The  
184 organic phase was evaporated to dryness under vacuum at 40°C and oil content  
185 determined gravimetrically. Fatty acid (FA) profile was determined using preparation  
186 of FA methyl esters, followed by gas chromatographic detection using standard  
187 method (AOAC, 2012).

188 Bulk density of the oil powder was measured using JEL jolting density metre  
189 (Gemini BV, Apeldoorn, Netherlands). Briefly, volume of a given mass of oil powder  
190 after 1250 taps was measured to calculate the tapped bulk density (Fitzpatrick, Iqbal,  
191 Delaney, Twomey, & Keogh, 2004).

192

### 193 2.5 Particle size measurement

194 A static light scattering instrument (Malvern MasterSizer 2000, Malvern Instruments  
195 Ltd, Worcestershire, UK) was used to determine the average droplet size and the  
196 overall size distribution of the emulsions before and after thermal cross-linking step.  
197 The relative refractive index (N) of the emulsion was 1.095, i.e. the ratio of the  
198 refractive index of soy oil (1.456) to that of the dispersion medium (1.33). The  
199 absorbance value of the emulsion particles was 0.001. The Sauter-mean diameter,  $d_{32}$

200  $(=\sum n_i d_i^3 / \sum n_i d_i^2)$  where  $n_i$  is the number of particles with diameter  $d_i$  of the emulsion  
201 droplets was measured. The average droplet size and the droplet size distribution of  
202 the emulsions were measured by dispersing in aqueous medium using Mie diffraction.  
203 The particle size of the oil powder was also analysed using static light scattering. In  
204 this case, the powder was dispersed at 3000 rpm for 5 min in medium chain  
205 triglycerides (MCT) and then analyzed by dispersing in MCT. All measurements were  
206 made at room temperature on at least three freshly prepared samples. Mean droplet  
207 diameter of the emulsions and particle diameters of oil powders were calculated as the  
208 average of five measurements.

209

#### 210 2.6 Determination of surface coverage

211 The surface coverage was measured using indirect method described by Srinivasan,  
212 Singh, & Munro (1996). Briefly, the emulsions before and after heat treatment were  
213 centrifuged at 45000 g for 40 min at 20 °C in a temperature-controlled centrifuge  
214 (Sorvall RC5C, DuPont Co., Wilmington, DE). The subnatants were carefully  
215 removed using a syringe and filtered sequentially through 0.45 and 0.22  $\mu\text{m}$  filters  
216 (Millipore Corp., Bedford, MA). The filtrates were analyzed for total protein using the  
217 Kjeldahl method (AOAC 981.10). The surface protein concentration ( $\text{mg}/\text{m}^2$ ) was  
218 calculated from the surface area of the oil droplets, determined by MasterSizer 2000,  
219 and the difference in the amount of protein used to prepare the emulsion and that  
220 measured in the filtered subnatants.

221

222

223

224

## 225 2.7 Confocal scanning laser microscopy (CSLM)

226 Oil powder was observed using Zeiss LSM 710 confocal microscope (Carl Zeiss  
227 MicroImaging GmbH, Jena, Germany), where the whey protein was stained using 0.1  
228 mL of 1.0% (w/v) Rhodamine 6G dye and imaged using  $\times 63$  objective at an  
229 excitation of 543 nm.

230

## 231 2.8 Morphology using scanning electron microscopy (SEM)

232 The particle morphology and internal microstructure of oil powder was  
233 characterized immediately after production as well as after 9 months of storage at 25  
234  $^{\circ}\text{C}$  in aluminum pouches. Oil powders were also characterized after removal of  
235 hexane extractable surface oil (Carneiro, Tonon, Grosso, & Hubinger, 2013). Briefly,  
236 oil powder was washed with hexane (1:10 w/w), shaken for 10 minutes followed by  
237 filtration of the powder using Whatman filter paper and the powder collected on the  
238 filter was rinsed three times with 20 mL of hexane. Oil powders with or without  
239 removal of surface oil were mounted on sample holders with double-side adhesive  
240 tape. A part of the sample was cut with a razor blade to reveal the inner structure of  
241 the particles. Samples were fixed with 1%  $\text{OsO}_4$  vapour during 24 hours.  
242 Visualization of samples was carried out in a Quanta 200F FEG microscope (FEI  
243 Company, Eindhoven, Netherlands), operated at 10 kV in low vacuum mode and  
244 equipped with a Backscatter Detector and no gold was sputtered. The samples were  
245 observed with wide range of magnifications of  $\times 1000$ ,  $\times 5000$  and  $\times 10,000$ .

246

## 247 2.9 Oil leakage using mechanical compression

248 Mechanical stability of oil powders was measured using a simple and reproducible  
249 method developed on the basis of underpinning principle of compaction force testing

250 of granulated powder (de Freitas Eduardo & da Silva Lannes, 2007). The amount of  
251 oil leaked out from the powder structure upon applying a compaction force was  
252 gravimetrically measured using a Texture Analyzer (TA XT PLUS, Stable Micro  
253 Systems, Ltd., UK) with a back extrusion A/BE assembly. Compression test was  
254 performed for freshly prepared oil powders as well as for the oil powders stored over  
255 a period of 15 months at 4 °C/ 70% RH conditions.

256 Oil powder (0.9 g) was filled into a cylindrical measuring cell and compressed by  
257 a compatible piston in a texture analyzer (probe, 20 mm diameter) (Bahtz, 2010). For  
258 each measurement, a layer of five filter papers (Whatman; 90 mm in diameter) was  
259 placed beneath the cylindrical measuring cell before filling with the oil powder  
260 sample. The piston was moved downward with a controlled speed of 0.5 mm/s and  
261 force of 30 N. The amount of oil leaked due to the mechanical compression and  
262 adsorbed to the filter papers (previously dried in a desiccator) was then determined  
263 gravimetrically by weighing the filter papers before and after the compression test.  
264 The oil leakage (%) represents the mass percentage of leaked oil related to the total oil  
265 present in the powder after compression. Mean value was calculated as average of  
266 five measurements for each oil powder formulation.

267

## 268 2.10 Measurement of lipid oxidation

269 For the oxidative stability tests, the oil powders without or with added antioxidants  
270 (300 ppm AP, 300 ppm AP + 1000 ppm M-TOC) were separately sealed in 50g  
271 aluminium pouches and amber glass vials (20 mL), and stored at 4 °C and 35 °C for  
272 20 weeks. For comparison, corresponding bulk oils (non-encapsulated) without or  
273 with added antioxidants were also stored under the same temperature conditions.  
274 Storage of oil powders at 35 °C was carried out as an accelerated storage test to

275 provide insights of oxidative stability for ambient storage. “1 week” at 35 °C is  
276 intended to be the equivalent to “1 month” of ambient storage conditions (18 °C) as  
277 expressed by Arrhenius equation (Taoukis & Labuza, 1996). The stored oils and oil  
278 powders were evaluated for oxidation by two distinct methods selected for primary  
279 and secondary oxidation products analyses (i.e. peroxide value and hexanal  
280 quantification using isotopic dilution method by headspace solid-phase  
281 microextraction (SPME) gas-chromatography mass-spectrometry, respectively).

282

#### 283 2.10.1 Peroxide value

284 Oil was extracted in the dark from the oil powders stored at 4 °C and 35 °C using the  
285 modified Folch cold extraction method as described before (Section 2.4). Peroxide  
286 value (PV) (meq/kg of oil) of the extracted oil and bulk oils was measured in six  
287 replicates by titration with 0.1 N sodium thiosulphate, using starch indicator  
288 according to AOCS Method Cd 8b-90 (AOCS, 1997).

289

#### 290 2.10.2 Hexanal determination in oil powder

291 Volatile (hexanal) was quantitatively determined following the method previously  
292 described by (Sarkar, et al., 2015). Briefly, oil powders and bulk oils previously  
293 weighed ( $2 \pm 0.01$ g) in 20 mL amber glass vials were spiked with hexanal-d<sub>12</sub> (120  
294 µg) as internal standard before the analysis. The GC-MS analyses were performed on  
295 a Thermo Finningan GC TOP 8000 equipped with a CTC PAL injector coupled to a  
296 Thermo Finningan Voyager quadrupole mass spectrometer (Brechtbühler Schlieren,  
297 Switzerland). A splitless injector with linear velocity of 30 mL/min and Helium as a  
298 carrier gas at constant pressure of 150 KPa were used. A DB-5MS (5% Phenyl 95%  
299 dimethylpolysiloxane, Brechtbühler, Schlieren, Switzerland) capillary column with 60

300 m length, 0.25 mm internal diameter and 0.25  $\mu\text{m}$  film thickness was employed. The  
301 column temperature was held at 50  $^{\circ}\text{C}$  for 10 min and increased to 250 $^{\circ}$  at 10 $^{\circ}\text{C}/\text{min}$   
302 and held for 10 min at this temperature. The temperatures of the ion source and  
303 transfer line were 200 and 220 $^{\circ}\text{C}$ , respectively. Electron impact mass spectra were  
304 recorded at 500 V in the 35-250 u mass range, at two scans/s. Volatiles were  
305 identified by usual MS-libraries. The concentration of volatiles was determined using  
306 calibration standard solutions in water containing hexanal and labeled hexanal  
307 (hexanal- $\text{d}_{12}$ ) as internal standards. The quantification was performed by plotting the  
308 peak area ratio of hexanal and hexanal- $\text{d}_{12}$  of the standard solution against the  
309 concentration ratio of hexanal and hexanal- $\text{d}_{12}$  determined in the sample in triplicate.  
310 The amount of hexanal (expressed in  $\mu\text{g}/\text{g}$ ) was calculated according to the following  
311 equation:

312

$$313 \quad \text{Content} = \frac{\left(\frac{A_A}{A_{IS}}\right) - I * m}{S * SW}$$

314 where, AA = area of hexanal in the sample, AIS = area of internal standard in sample,  
315 I = intercept of the calibration curve's equation, S = slope of the calibration's curve  
316 equation, m = amount of internal standard ( $\mu\text{g}$ ) and SW = sample weight (g). Mean  
317 value is the average of triplicate measurements.

318 in oil against internal standard (hexanal- $\text{d}_{12}$ ). Analyses of hexanal in headspace were  
319 performed in triplicate.

320

321

322

323

324 2.11 Statistical analyses

325 The results were statistically analyzed by analysis of variance (ANOVA) using  
326 Graphpad 5 Prism software and differences were considered significant when  $p < 0.05$   
327 were obtained.

328

### 329 **3 Results and discussion**

#### 330 3.1 Characteristics of oil powder

331 Figure 1 shows the visual aspect of the resulting dry granular oil powder after the  
332 spray drying of the thermally cross-linked oil-in-water emulsions. The oil powder had  
333 a light texture and did not have any stickiness or evidence of oil leakage even after  
334 several months of storage at a macroscopic level. However, on shearing between  
335 fingers or between the oral palate in the mouth, the oil phase was gradually released  
336 giving a creamy tactile/ mouth feel. As presented in Table 1, the oil powder had 0.21  
337 wt% moisture content. Ultra-high quantities of oil of 95.3 wt% were encapsulated in  
338 the powder. The experimental oil/protein ratio in resulting oil powder (26.1) agreed  
339 reasonably well with the theoretical oil/protein ratio in the starting emulsions (25.5).  
340 This close agreement of data also confirms the precision of the cold Folch extraction  
341 method for complete extraction, where the use of high shear played a significant role  
342 to break the wall of encapsulated material and liberate the oil from the cross-linked  
343 whey protein matrix. As expected, the fatty acid analysis of the oil powder  
344 corresponded to that of soy oil (Sarkar, et al., 2015), suggesting no change in the oil  
345 composition during oil powder formation and/or extraction. The bulk density of the  
346 oil powder was 0.44 g/ cc, which is within the range of high fat milk powders  
347 (Sharma, Jana, & Chavan, 2012).

348

### 349 3.2 Particle size of emulsions and oil powder

350 Emulsification, cross-linking and spray drying are the three key steps in the  
351 preparation of this ultra-high content oil powder (Figure 1). The droplet size  
352 distributions of the 20 wt% oil-in-water emulsions prior to, after the heat treatment  
353 process and particle size distribution of the resulting oil powder are shown in Figure  
354 2. The emulsions formed by homogenisation at 400/100 bars had a monomodal  
355 droplet size distribution with the majority of droplets being in the range of 0.1-4.0  
356  $\mu\text{m}$ , with an average droplet size ( $d_{32}$ ) of  $\sim 0.38 \mu\text{m}$  (Table 2). As expected at pH 7,  
357 which is sufficiently above the pI of whey protein, the whey proteins at the interface  
358 had a net negative charge that was sufficient to prevent the emulsions from  
359 flocculation through strong electrostatic repulsive forces.

360 After the thermal cross-linking treatment at  $82 \text{ }^\circ\text{C}/ 10$  minutes, the emulsions  
361 showed a slightly wider size distribution compared with the parent emulsions, ranging  
362 from 0.1 to  $10 \mu\text{m}$ , with an increased  $d_{32}$  value of  $0.67 \mu\text{m}$ . There was no significant  
363 difference between the  $d_{32}$  value of the cross-linked emulsion and the emulsion before  
364 heat treatment ( $p > 0.05$ ). The cross-linked emulsions were homogenous and  
365 kinetically stable showing no flocculation during the period of study. The surface  
366 protein coverage increased from  $\sim 1.1$  to  $\sim 2.1 \text{ mg/m}^2$  on thermal treatment of the  
367 emulsions (data not shown). The significant increase in total surface protein coverage  
368 of whey-protein-stabilized emulsions on thermal treatment is in agreement with the  
369 results of previous workers (Monahan, McClements, & German, 1996; Sliwinski et  
370 al., 2003; Jiménez-Flores, Ye, & Singh, 2005). This suggests that intra-droplet  
371 protein-protein interactions were favoured in our study than inter-droplet flocculation,  
372 resulting in a sufficiently cohesive and elastic adsorption layer at the interface  
373 (Monahan, McClements, & German, 1996; Romoscanu & Mezzenga, 2005). Upon

374 spray drying, the oil powder showed a monomodal distribution and an average droplet  
375 size ( $d_{32}$ ) of  $\sim 37 \mu\text{m}$  and thus was around 50 times larger than the individual cross-  
376 linked emulsion oil droplets. The oil powder had partial redispersibility in water after  
377 reconstitution, which was also highlighted by Mezzenga & Ulrich (2010). This might  
378 be attributed to the ultrahigh content of hydrophobic phase and possible presence of  
379 surface oil. Hence, droplet size in the powdered emulsions after reconstitution in  
380 water could not be measured with accuracy and hence not reported.

381 To understand the effect of drying on the emulsion droplet size, CLSM was  
382 employed. The CSLM of the oil powder (Figure 3A), which was labelled with protein  
383 stain (Rhodamine 6G) showed that the oil powder granules were of a variety of size.  
384 Each oil powder granule contained oil droplets separated by a very thin layer of  
385 protein film. The oil droplets located within the powder matrix as observed in CSLM  
386 images were uniform small droplets evenly distributed within the cross-linked  
387 viscoelastic protein matrix. A relatively small proportion of large droplets observed  
388 within the powder in the CLSM images could be attributed to the droplet coalescence  
389 owing to shear induced rupture of the interfacial layer during the rotary atomisation  
390 step (Jafari, et al., 2008; Taneja, et al., 2013). It is worth noting here that the  
391 emulsions stabilized by whey protein monolayer alone at this oil/protein ratio without  
392 the thermal cross-linking step could not withstand the spray drying conditions and  
393 oiled off dramatically. This indicates that the cross-linked protein shell was essential  
394 to stabilize the individual droplets against droplet coalescence.

395 Interestingly, as observed in the higher magnification image (Figure 3B); the  
396 protein shell enveloping each powder granule was comparatively thicker than the  
397 protein layers surrounding each individual oil droplets within the powder granule.  
398 This is expected due to the surface-activity-led diffusion and subsequent adsorption of

399 the excess non-adsorbed protein at the air-water interface of the powder during the  
400 final stages of water evaporation during spray drying (Adhikari, Howes, Bhandari, &  
401 Langrish, 2009; Mezzenga, et al., 2010). During spray drying and the associated mass  
402 transfer, the water in the continuous phase of the emulsions moves along a  
403 concentration gradient towards the surface (Jones et al., 2013; Kim, Chen, & Pearce,  
404 2009). As it can expected, water being small molecule diffused faster and carried with  
405 it larger whey protein molecules present in the continuous phase, which cannot  
406 diffuse as quickly in the opposite direction. The emulsified oil and adsorbed protein  
407 were also carried along in the convective flux of water moving toward the surface.  
408 This movement continued until the continuous phase became relatively immobile and  
409 underwent shrinkage thereafter as the water evaporated. Hence, it appears that whey  
410 protein concentration of 3.6 wt% was sufficient to stabilise the emulsion (~ 55%  
411 adsorption ratio, data not shown) as well as had non-adsorbed protein contributing to  
412 the surface stabilization of drying droplets.

413

### 414 3.3 Influence of emulsion droplet size on mechanical stability of oil powder

415 During the use of the oil powder in real industrial line for manufacturing of  
416 various product applications, the oil powder would essentially be subjected to  
417 different levels of mechanical stresses. Depending on the applied stress, one could  
418 anticipate that the protective cross-linked protein shell could be weakened, and above  
419 a critical level, it might be ruptured, leading to the leakage of the encapsulated  
420 emulsified oil droplets. Therefore, the mechanical stability of the oil powder was  
421 investigated by quantitatively measuring the oil leakage under normal compression  
422 (Bahtz, 2010).

423 To understand the effect of droplet size of parent emulsion on powder particle size  
424 and mechanical stability of the resulting oil powders, the homogenization pressure  
425 was varied to create emulsions of a range of size distributions (Table 2). With the  
426 same ratio of oil/protein, the increase of homogenization pressure in the range of 100–  
427 1200 bars led to a steady reduction of average oil droplet size ( $d_{32}$  values between  
428 ~2.31 and 0.21  $\mu\text{m}$ , respectively). This decrease in oil droplet size was due to the  
429 higher levels of shear forces associated with increased homogenizing pressure applied  
430 (Hogan, McNamee, O'Riordan, & O'Sullivan, 2001).

431 As shown in Table 2, varying emulsion droplet size before drying did not have a  
432 significant influence on powder particle diameter ( $p > 0.05$ ), which is in agreement  
433 with findings of previous studies (Danviriyakul, McClements, Decker, Nawar, &  
434 Chinachoti, 2002; Ye, Anema, & Singh, 2007). However, the level of oil leakage on  
435 mechanical compression decreased significantly with decreasing oil droplet size until  
436 0.38  $\mu\text{m}$  ( $p < 0.05$ ). This is in line with previous study, which shows that droplet  
437 diameter has a significant effect on burst strength during compression testing, with  
438 smaller capsules sustaining higher stresses before bursting out (Keller & Sottos,  
439 2006). However, when the  $d_{32}$  of the emulsion droplets further decreased to 0.21  $\mu\text{m}$   
440 at a homogenization pressure of 1200  $\times$  100 bars, the surface area increased  
441 significantly and the available whey protein might not have been sufficient to coat the  
442 increased surface area of droplets generated. Thus increase of oil leakage to 2.7% was  
443 observed.

444 In the long-term stability experiments, research focusses on oil powder, which  
445 was prepared using 0.38  $\mu\text{m}$  sized emulsion droplets (400/ 100 bar pressure) as it had  
446 the least oil leakage.

447

#### 448 3.4 Long-term mechanical stability of oil powder

449 To investigate the long-term mechanical stability, oil powder stored at 4 °C for a  
450 period of 9 months was tested for oil leakage. As shown in Figure 4, the kinetics of oil  
451 leakage followed three-stage behaviour. There was a slow increase in the degree of oil  
452 leakage until 5 months. Then, both the kinetics and extent of oil leakage increased  
453 significantly until the end of 9 months followed by a plateau thereafter. Even after  
454 long storage time of 15 months, the powder did not show more than 10 wt% of oil  
455 leakage on compaction. The behaviour upto 5 months might be attributed to the  
456 gradual leakage of the surface oil being present. With subsequent storage and inter-  
457 particle friction, there might be rupture of the protein matrix and oil might have oozed  
458 out of the capillaries (if any) during the 5-9 months period, which might have resulted  
459 in such rapid rate of oil leakage.

460 To understand the microstructure at a deeper length scale, SEM allowed  
461 investigation of the internal and external morphologies of the oil powders after  
462 production as well as after storage (Figure 5). Analysing the external morphology  
463 (Figure 5A), oil powder granules of a variety of sizes showed a spherical shape,  
464 smooth surface with no apparent visible cracks or fissures. As compared to previous  
465 literatures (Gallardo, et al., 2013; Jafari, et al., 2008), the appearance of characteristic  
466 concave surface on oil powder as a result of spray drying was not observed in our  
467 study, which might be expected due to substantially higher oil content.

468 Although there was no visible appearance of free oil or stickiness at the  
469 macroscopic level, the surface of the oil powder at the microscopic length scale  
470 showed coverage by a layer of oil and also showed “free oil droplets” at the surface. It  
471 can be argued that these layers of oil were causing inter-particle bridge formation and  
472 (Figure 5A) might have covered any surface cracks or fissures if at all generated. As

473 observed in Figure 5B, the stored sample did not show any visual deterioration or  
474 irregularities of structure in terms of emergence of any pores, surface cracks or  
475 wrinkling. However, surface oil layer and appearances of “free oil droplets” were  
476 further enhanced upon storage (Figure 5B). This suggests that the comparatively  
477 higher surface oil available as a function of storage was easier to ooze out of the  
478 structure when subjected to mechanical compaction.

479 The higher magnification images of the internal morphology of the powder with  
480 or without storage (Figures 5B and B’) showed less hollowed structure as compared  
481 to typical characteristic powder particles obtained in spray drying with higher wall  
482 material content. As expected, the structure was supersaturated with oil (> 95%)  
483 embedded throughout the oil matrix and the microstructure had some resemblance  
484 with cream powder with 75 wt% oil content as observed by Kim, Chen, & Pearce,  
485 (2002).

486 Although there is no clear definition of “surface oil” particularly in this new class  
487 of spray dried emulsions with ultra-high oil loads, we can consider it as the hexane  
488 extractable oil. This is basically a combination of “free oil” located at the powder  
489 surface, oozed out of the cracks or capillaries formed during drying process,  
490 insufficiently emulsified oil, coalesced droplets within the powder (Drusch & Berg,  
491 2008; Moisisio, et al., 2014) as well as the oil extracted due to the potential hexane-  
492 induced breakdown of the hydrophobic protein linkages in the cross-linked whey  
493 protein matrix. Hence, to gain deeper microstructure insights, it was interesting to  
494 observe the powder after removal of the “hexane extractable” surface oil (Figure 6).

495 As shown in Figure 6A, the removal of surface oil resulted in dramatic shrinkage  
496 of the oil powder granules with clear appearances of wrinkles, dents and open pores.  
497 A cross cut of the internal morphology clearly indicated a porous “sponge” like

498 microstructure with deformation of the closely packed oil droplets into polyhedral  
499 shapes (Figure 6B). The microstructure showed some larger voids, which might be  
500 resulting from hexane-extraction of larger coalesced droplets formed either due to  
501 spray drying as seen in CLSM images and also due to the rupture of protein layer due  
502 to inter-granular friction on storage (Andersson & Bergström, 2005). Overall, this  
503 microstructural evidence together with the quantitative increase of oil leakage as a  
504 function of storage suggests that our initial hypothesis of “crosslinked protein film  
505 being capable of protecting the encapsulated oil against leakage” cannot be fully  
506 validated. Although interfacial cross-linking forms a cohesive film and enables spray  
507 drying effectively, the film is not sufficiently dense to completely coat the particle  
508 surface, sustain inter-granular friction and protect the encapsulated oil fully from  
509 leakage on mechanical compression.

510

### 511 3.5 Long-term oxidative stability of oil powder

512 Oxidative stability study of oil powder and corresponding bulk oils was carried out at  
513 4 °C and 35 °C, respectively as a function of storage time of 5 months. In an industrial  
514 context, many if not most bulk oils contain antioxidants such as AP or M-TOC being  
515 added at the suppliers’ end to restrict oxidative deterioration. Furthermore, synergistic  
516 effects of antioxidants such as AP and M-TOC in microencapsulated system have  
517 been well studied (Velasco, et al., 2000). Hence, in this set of experiments, oil  
518 powders were produced with added 300 ppm AP or a combination of 300 ppm AP  
519 and 1000 ppm M-TOC. As one might anticipate, the bulk oil (unprocessed) and the  
520 encapsulated oil fraction (oil extracted from oil powder) displayed different oxidative  
521 behaviour. While the free oil oxidized as lipids in continuous phase, oxidation in the

522 encapsulated emulsified oil powder was the result of individual oil droplets oxidizing  
523 at different reaction rates.

524 At 4 °C, PV values of both bulk oil and oil powder with or without any added  
525 antioxidants did not show any exceptional increase ( $\leq 2.0$  meq O<sub>2</sub>/ kg oil) over the  
526 long term storage period of 5 months (Figure 7A). The PV at which soybean oil is  
527 unacceptable from a sensory standpoint has been reported to be 2.0 meq O<sub>2</sub>/ kg oil  
528 (Hawrysh, 1990). Hence, it seems that oil powder without added antioxidant can be  
529 stored for 20 weeks without a sharp evolution of hydroperoxides and be still  
530 acceptable when stored at 4°C. Furthermore, the PV value was significantly lower  
531 than that provided in CODEX STAN 210 for refined vegetable oils, where acceptance  
532 limit for PV is 10 meq O<sub>2</sub>/ kg oil. However, oil powders had a significantly higher  
533 rate and extent of oxidation than the corresponding bulk oil even at 4°C ( $p < 0.05$ ). The  
534 comparison of oil powder and bulk oil containing antioxidants also elucidated some  
535 interesting features (Figure 7A). Addition of AP ( $p < 0.05$ ) or AP+M-TOC ( $p < 0.01$ )  
536 resulted in significant retardation of generation of hydroperoxides in the bulk oil.  
537 However, such beneficial effects of addition of antioxidants were not observed in case  
538 of the oil powder.

539 At 35 °C (Figure 7B), the PV value increased markedly during the storage for  
540 both oil powder (54.2 meq O<sub>2</sub>/ kg oil) and corresponding bulk oil (38.5 meq O<sub>2</sub>/ kg  
541 oil). In case of the bulk oils, addition of AP+M-TOC was considerably more effective  
542 to prevent the evolution of hydroperoxides above 2.1 meq O<sub>2</sub>/ kg oil as compared to  
543 AP alone ( $p < 0.05$ ) on storage for 5 months. On the other hand, oil powders resulted  
544 in faster oxidation kinetics and higher extent of evolution of hydroperoxides (37.2  
545 meq O<sub>2</sub>/ kg oil for AP, 48.4 meq O<sub>2</sub>/ kg oil for AP+ M-TOC) irrespective of their  
546 antioxidant types at 35°C (Figure 7B).

547 It is worth recognizing that hydroperoxides generated in oil powder was nearly  
548 three-fold higher as compared to the corresponding bulk oil at the start of the storage  
549 test. This higher extent of hydroperoxides generation in the oil powders at the  
550 beginning of the storage study might be expected due to the increased rate of exposure  
551 of oil to oxygen, light and higher temperature during multi-step production process of  
552 oil powder (i.e. homogenization, thermal treatment, atomization of the feed emulsion  
553 followed by spray drying) (Baik et al., 2004, Velasco et al., 2000). In addition, the  
554 processing generates oil droplets and thus a huge surface area increasing the degree of  
555 oxidation.

556 One might argue that the cross-linked whey protein film, which is the central  
557 concept in this new class of oil powder, was not sufficiently dense enough to provide  
558 complete oxygen or light barrier properties to the encapsulated oil. As shown in  
559 Figure 8, there existed a strong linear correlation between level of hydroperoxides  
560 generated in the oil powder at and oil leakage (%) during the same periods of storage  
561 at 4 °C ( $r^2=0.92$ ). At 35 °C, there existed an exponential relationship between the  
562 mechanical and oxidative stability ( $r^2=0.95$ ). This further highlights that the higher  
563 level of oxidative deterioration in case of oil powder was not only driven by the  
564 multistep production process but also by the rather porous microstructure of oil  
565 powder as well as weaker films incapable of providing sufficient oxygen and light  
566 barrier properties.

567 Although PV provides insights on primary oxidation, the hydroperoxides that  
568 might have been converted to secondary oxidation products are generally more  
569 informative from off flavour generation and rancidity perspective. To quantify the  
570 generation of secondary oxidation products, Figures 9A and B shows the evolution of  
571 hexanal concentration ( $\mu\text{g/g}$  or ppm) of the oil powders and corresponding bulk oils

572 stored at 4 °C and 35 °C, respectively as function of 5 months' storage time. Hexanal  
573 has proved to be a suitable marker for the evaluation of the oxidative status of oil  
574 containing linoleic acid, as hexanal is formed from both 9- and 13-hydroperoxides of  
575 linoleate and from other unsaturated aldehydes during the oxidation of linoleate  
576 (Sarkar, et al., 2015). Since soy oil contained significant amounts of linoleic acid  
577 (Table 1), hexanal was identified as a suitable marker for studying the secondary  
578 oxidation of the oil powders as a basis for comparison. The higher quantity of hexanal  
579 generated can be regarded as a measure of poor sensorial quality. Based on  
580 preliminary oxidative stability study (Sarkar, et al., 2015) and sensory tests (data not  
581 shown), hexanal generated higher than 1 ppm was considered to be the critical limit to  
582 identify any off flavor generation.

583 At 4 °C (Figure 9A), the bulk oils with and without added antioxidant behaved  
584 similarly in terms of evolution of hexanal ( $p>0.05$ ). The evolution of hexanal in bulk  
585 oils was much slower and lesser in magnitude than that of corresponding oil powders  
586 at 4 °C ( $p<0.05$ ). Interestingly, AP appeared to have slight protective effect in oil  
587 powder keeping the hexanal evolution below 1 ppm over the period of study at 4 °C.  
588 As it can be expected, at 35 °C, both oil and oil powder showed higher extent of  
589 hexanal evolution (5.6 ppm and 5.3 ppm respectively) ( $p>0.05$ ). Although addition of  
590 antioxidants had a pronounced protective effect on bulk oils ( $p<0.05$ ), such  
591 antioxidant effects were not observed in oil powder. Ascorbyl palmitate (AP) slightly  
592 retarded the oxidation kinetics in oil powder as compared to oil powder without any  
593 added antioxidants. On the other hand, presence of M-TOC accelerated the oxidation  
594 kinetics and extent in case of oil powder. The poor effect of M-TOC might be due to  
595 the high levels of tocopherols already present in the soy oil used in the systems and  $\alpha$ -

596 tocopherol being known to have prooxidative effects in high concentrations  
597 (Jacobsen, Let, Nielsen, & Meyer, 2008).

598       It should be noted that surface area of the oil powder is significantly higher than  
599 the surface area of the corresponding bulk oils. One would therefore expect higher  
600 lipid oxidation kinetics in this kind of emulsion based encapsulated system as  
601 compared to the corresponding bulk oils. In general, the slowing down of such  
602 deteriorative lipid oxidation reactions in encapsulated powders is largely dependent  
603 on the ability of the encapsulant to keep the oxidizable lipid substrates in the emulsion  
604 droplet core (i.e. hydroperoxides generated) well segregated from aqueous phase pro-  
605 oxidants (e.g. metals) (Waraho, McClements, & Decker, 2011). It also depends on the  
606 ability of the encapsulant to enable lesser oxygen diffusion to the encapsulated oil  
607 droplets during storage, thus contributing to longer ingredient shelf life. Furthermore,  
608 emulsifier such as whey proteins are known to provide antioxidant effect on the  
609 emulsified oil through availability of free sulfhydryl groups (Faraji, McClements, &  
610 Decker, 2004; Tong, Sasaki, McClements, & Decker, 2000).

611       In our study, although thermal treatment might have generated reactive sulfhydryl  
612 groups, they were possibly involved in formation of disulphide linkages during  
613 creation of cross-linked interfacial film and might not be available to exert the  
614 antioxidant effect. It is also noteworthy that although a cohesive film was formed at  
615 the droplet interface due to the thermal crosslinking of whey protein, it might be still  
616 permeable to proactive species such as iron. This is in line with the results of  
617 enzymatically cross-linked sodium caseinate film at oil-water interface, where the  
618 inability to restrict pro-oxidants promoted the decomposition of hydroperoxides into  
619 free radicals that further oxidized the unsaturated fatty acids in the emulsion droplet  
620 core (Kellerby, Gu, McClements, & Decker, 2006). Moreover, the highly porous

621 microstructure (as observed in Figure 6) possibly allowed oxygen, free radicals  
622 generated or prooxidants in the aqueous phase to diffuse through the emulsion droplet  
623 interface where they reacted with the oil inside the droplets. This resulted in faster  
624 oxidation kinetics which is in agreement with literatures showing higher degree of  
625 lipid oxidation in encapsulated as compared to non-encapsulated systems (Kellerby, et  
626 al., 2006). The increased level of lipid oxidation in oil powder during storage  
627 indicates that the matrix to encapsulated oil ratio of 1:25 seems to be not sufficient to  
628 prevent diffusion of oxygen during storage of the oil powders. Hence, besides the  
629 processing aspects of oil powder, the kind of microstructure generated during oil  
630 powder production, significantly contributed to enhance lipid oxidation as compared  
631 to the bulk oils (unprocessed).

632 It is worth noting here that this study is not sufficient to identify the technological  
633 conditions, which promote or inhibit the lipid oxidation rate in the oil powder when it  
634 is present in the final product applications. For instance, the presence of pro-oxidants  
635 in the formulation of the finished product applications, water activity, processing  
636 conditions during the manufacturing of the products (e.g. heat treatment, mechanical  
637 shear), product packaging and storage conditions are supposed to dramatically impair  
638 the stability of encapsulated oil powders. Contrastingly, presence of natural  
639 antioxidants in the application recipe might retard lipid oxidation. For these reasons, a  
640 systematic storage test (trained sensory panel analysis) of the final product  
641 applications containing oil powder with or without added antioxidants needs to be  
642 performed to clearly predict a more complete picture of the oxidative stability of the  
643 oil powders when used as a fat replacer in the finished product applications.  
644 Furthermore, quantitatively describing the mechanism of lipid oxidation in this type

645 of oil powders with ultra-high oil content because of processing and/or  
646 microstructural aspect needs to be elucidated in future.

647

## 648 **Conclusions**

649 Our study showed a scaled up approach to create spray dried emulsions with ultra-  
650 high oil loading of 95.3 wt%. The cross-linking of the interfacial layer enabled spray  
651 drying of the emulsion droplets without the requirement of any additional wall  
652 materials. The initial emulsion droplets size influenced the mechanical stability of the  
653 oil powder as evidenced by oil leakage upon compaction. Our study also established  
654 an easier approach to study mechanical stability of oil powder in an industrial context.  
655 The oil leakage upon compression during storage was due to not only the surface oil  
656 but also coalesced oil droplets formed during spray drying as well as inter-granular  
657 friction in the capillaries oozing out of the porous “sponge”-like permeable  
658 microstructure of the oil powder as seen in the SEM. The processing aspects of oil  
659 powder (e.g. homogenization, thermal cross-linking and spray drying) aggravated the  
660 lipid oxidation kinetics as compared to the unprocessed bulk oils. Furthermore, the  
661 cohesive cross-linked whey protein film in absence of any added glassy matrix was  
662 not sufficiently dense to protect the oil from oxidation and allowed diffusion of  
663 oxygen and prooxidants during storage period. The insights generated in designing  
664 this “sponge” like porous microstructure and the microscopic detailing of the  
665 mechanism of instability is expected to serve as a reference for the designing of new  
666 class of microstructures for use in food, pharmaceutical, personal care and home care  
667 industries.

668

## 669 **Acknowledgements**

670 Authors are very grateful to Dr. Eric Kolodziejczyk and Ms. Martine Rouvet, who  
671 produced the confocal and scanning electron micrographs and to Ms. Alina Hevér for  
672 peroxide value determination shown in this study.

673

## 674 **References**

675 Adhikari, B., Howes, T., Bhandari, B. R., & Langrish, T. A. G. (2009). Effect of  
676 addition of proteins on the production of amorphous sucrose powder through  
677 spray drying. *Journal of Food Engineering*, 94(2), 144-153.

678 Andersson, K. M., & Bergström, L. (2005). Friction and adhesion of single spray-  
679 dried granules containing a hygroscopic polymeric binder. *Powder*  
680 *Technology*, 155(2), 101-107.

681 AOAC. (1995). *Official methods of analysis of Association of Official Analytical*  
682 *Chemists*, Washington, DC, USA.

683 AOAC. (2012). *Determination of labeled fatty acid contents in milk products and*  
684 *infant formula - capillary gas chromatography*. AOAC First Action 2012.13.  
685 *Official methods of analysis of Association of Official Analytical Chemists*,  
686 *Washington, DC, USA*.

687 AOCS. (1997). *Official methods and recommended practices of the American Oil*  
688 *Chemists' Society*, 5th edition. Champaign, UK.

689 Bahtz, J. (2010). *Fats in dough application: Assessment of process alternatives*.  
690 *Diploma Thesis at Technische Universität Berlin, Germany and Nestlé*  
691 *Research Centre Lausanne, Switzerland*.

- 692 Cameron, N. R. (2005). High internal phase emulsion templating as a route to well-  
693 defined porous polymers. *Polymer*, 46(5), 1439-1449.
- 694 Carneiro, H. C. F., Tonon, R. V., Grosso, C. R. F., & Hubinger, M. D. (2013).  
695 Encapsulation efficiency and oxidative stability of flaxseed oil  
696 microencapsulated by spray drying using different combinations of wall  
697 materials. *Journal of Food Engineering*, 115(4), 443-451.
- 698 Danviriyakul, S., McClements, D. J., Decker, E., Nawar, W. W., & Chinachoti, P.  
699 (2002). Physical stability of spray-dried milk fat emulsion as affected by  
700 emulsifiers and processing conditions. *Journal of Food Science*, 67(6), 2183-  
701 2189.
- 702 de Freitas Eduardo, M., & da Silva Lannes, S. C. (2007). Use of texture analysis to  
703 determine compaction force of powders. *Journal of Food Engineering*, 80(2),  
704 568-572.
- 705 Dionisi, F., Golay, P. A., Aeschlimann, J. M., & Fay, L. B. (1998). Determination of  
706 cholesterol oxidation products in milk powders: Methods comparison and  
707 validation. *Journal of Agricultural and Food Chemistry*, 46(6), 2227-2233.
- 708 Drusch, S., & Berg, S. (2008). Extractable oil in microcapsules prepared by spray-  
709 drying: Localisation, determination and impact on oxidative stability. *Food*  
710 *Chemistry*, 109(1), 17-24.
- 711 Euston, S. R., Finnigan, S. R., & Hirst, R. L. (2000). Aggregation kinetics of heated  
712 whey protein-stabilized emulsions. *Food Hydrocolloids*, 14(2), 155-161.

713 Faraji, H., McClements, D. J., & Decker, E. A. (2004). Role of continuous phase  
714 protein on the oxidative stability of fish oil-in-water emulsions. *Journal of*  
715 *Agricultural and Food Chemistry*, 52(14), 4558-4564.

716 Fitzpatrick, J. J., Iqbal, T., Delaney, C., Twomey, T., & Keogh, M. K. (2004). Effect  
717 of powder properties and storage conditions on the flowability of milk  
718 powders with different fat contents. *Journal of Food Engineering*, 64(4), 435-  
719 444.

720 Gallardo, G., Guida, L., Martinez, V., López, M. C., Bernhardt, D., Blasco, R.,  
721 Pedroza-Islas, R., & Hermida, L. G. (2013). Microencapsulation of linseed oil  
722 by spray drying for functional food application. *Food Research International*,  
723 52(2), 473-482.

724 **Hamann, F., & Schmid, M. (2014). Determination and quantification of molecular**  
725 **interactions in protein films: A review. *Materials*, 7(12), 7975-7996.**

726 Hogan, S. A., McNamee, B. F., O'Riordan, E. D., & O'Sullivan, M. (2001).  
727 Microencapsulating properties of sodium caseinate. *Journal of Agricultural*  
728 *and Food Chemistry*, 49(4), 1934-1938.

729 Ixtaina, V. Y., Julio, L. M., Wagner, J. R., Nolasco, S. M., & Tomás, M. C. (2015).  
730 Physicochemical characterization and stability of chia oil microencapsulated  
731 with sodium caseinate and lactose by spray-drying. *Powder Technology*,  
732 271(0), 26-34.

733 Jacobsen, C., Let, M. B., Nielsen, N. S., & Meyer, A. S. (2008). Antioxidant  
734 strategies for preventing oxidative flavour deterioration of foods enriched with

735 n-3 polyunsaturated lipids: a comparative evaluation. Trends in Food Science  
736 & Technology, 19(2), 76-93.

737 Jafari, S. M., Assadpoor, E., Bhandari, B., & He, Y. (2008). Nano-particle  
738 encapsulation of fish oil by spray drying. Food Research International, 41(2),  
739 172-183.

740 Jiménez-Flores, R., Ye, A., & Singh, H. (2005). Interactions of whey proteins during  
741 heat treatment of oil-in-water emulsions formed with whey protein isolate and  
742 hydroxylated lecithin. Journal of Agricultural and Food Chemistry, 53(10),  
743 4213-4219.

744 Jones, J. R., Prime, D., Leaper, M. C., Richardson, D. J., Rielly, C. D., & Stapley, A.  
745 G. F. (2013). Effect of processing variables and bulk composition on the  
746 surface composition of spray dried powders of a model food system. Journal  
747 of Food Engineering, 118(1), 19-30.

748 Keller, M. W., & Sottos, N. R. (2006). Mechanical Properties of Microcapsules Used  
749 in a Self-Healing Polymer. Experimental Mechanics, 46(6), 725-733.

750 Kellerby, S. S., Gu, Y. S., McClements, D. J., & Decker, E. A. (2006). Lipid  
751 oxidation in a menhaden oil-in-water emulsion stabilized by sodium caseinate  
752 cross-linked with transglutaminase. Journal of Agricultural and Food  
753 Chemistry, 54(26), 10222-10227.

754 Kim, E. H. J., Chen, X. D., & Pearce, D. (2002). Surface characterization of four  
755 industrial spray-dried dairy powders in relation to chemical composition,  
756 structure and wetting property. Colloids and Surfaces B: Biointerfaces, 26(3),  
757 197-212.

758 Kim, E. H. J., Chen, X. D., & Pearce, D. (2009). Surface composition of industrial  
759 spray-dried milk powders. 2. Effect of spray drying conditions on the surface  
760 composition. *Journal of Food Engineering*, 94(2), 169-181.

761 Mezzenga, R., & Ulrich, S. (2010). Spray-Dried Oil Powder with Ultrahigh Oil  
762 Content. *Langmuir*, 26(22), 16658-16661.

763 Moisisio, T., Damerou, A., Lampi, A.-M., Piironen, V., Forssell, P., & Partanen, R.  
764 (2014). Interfacial protein engineering for spray-dried emulsions – Part I:  
765 Effects on protein distribution and physical properties. *Food Chemistry*,  
766 144(0), 50-56.

767 Monahan, F. J., McClements, D. J., & German, J. B. (1996). Disulfide-mediated  
768 polymerization reactions and physical properties of heated WPI-stabilized  
769 emulsions. *Journal of Food Science*, 61(3), 504-509.

770 Nikiforidis, C. V., & Scholten, E. (2015). High internal phase emulsion gels (HIPE-  
771 gels) created through assembly of natural oil bodies. *Food Hydrocolloids*,  
772 43(0), 283-289.

773 Patel, A. R., Rodriguez, Y., Lesaffer, A., & Dewettinck, K. (2014). High internal  
774 phase emulsion gels (HIPE-gels) prepared using food-grade components. *RSC*  
775 *Advances*, 4(35), 18136-18140.

776 Romoscanu, A. I., & Mezzenga, R. (2005). Cross linking and rheological  
777 characterization of adsorbed protein layers at the oil–water interface.  
778 *Langmuir*, 21(21), 9689-9697.

- 779 Romoscanu, A. I., & Mezzenga, R. (2006). Emulsion-templated fully reversible  
780 protein-in-oil gels. *Langmuir*, 22(18), 7812-7818.
- 781 Sarkar, A., Golay, P.-A., Acquistapace, S., & Craft, B. D. (2015). Increasing the  
782 oxidative stability of soybean oil through fortification with antioxidants.  
783 *International Journal of Food Science & Technology*, 50(3), 666-673.
- 784 Sharma, A., Jana, A. H., & Chavan, R. S. (2012). Functionality of milk powders and  
785 milk-based powders for end use applications—A review. *Comprehensive*  
786 *Reviews in Food Science and Food Safety*, 11(5), 518-528.
- 787 Sliwinski, E. L., Roubos, P. J., Zoet, F. D., van Boekel, M. A. J. S., & Wouters, J. T.  
788 M. (2003). Effects of heat on physicochemical properties of whey protein-  
789 stabilised emulsions. *Colloids and Surfaces B: Biointerfaces*, 31 (1-4), 231-  
790 242.
- 791 Srinivasan, M., Singh, H. & Munro, P. A. (1996). Sodium-caseinate stabilised  
792 emulsions: Factors affecting coverage and composition of surface proteins.  
793 *Journal of Agricultural and Food Chemistry*, 44 (12), 3807-3811.
- 794 Taneja, A., Ye, A., Jones, J. R., Archer, R., & Singh, H. (2013). Behaviour of oil  
795 droplets during spray drying of milk-protein-stabilised oil-in-water emulsions.  
796 *International Dairy Journal*, 28(1), 15-23.
- 797 Taoukis, P. S., & Labuza, T. P. (1996). Integrative concepts. In O. Fennema (Ed.),  
798 *Food Chemistry* (pp. 1013-1042). New York, USA: Marcel Dekker.

799 Tolkach, A., & Kulozik, U. (2007). Reaction kinetic pathway of reversible and  
800 irreversible thermal denaturation of  $\beta$ -lactoglobulin. *Lait*, 87(4-5), 301-  
801 315.

802 Tong, L. M., Sasaki, S., McClements, D. J., & Decker, E. A. (2000). Antioxidant  
803 activity of whey in a salmon oil emulsion. *Journal of Food Science*, 65(8),  
804 1325-1329.

805 Ubbink, J., & Krüger, J. (2006). Physical approaches for the delivery of active  
806 ingredients in foods. *Trends in Food Science & Technology*, 17(5), 244-254.

807 Velasco, J., Dobarganes, M. C., & Márquez-Ruiz, G. (2000). Oxidation of free and  
808 encapsulated oil fractions in dried microencapsulated fish oils. *Grasas y*  
809 *Aceites*, 51(6), 439-446.

810 Waraho, T., McClements, D. J., & Decker, E. A. (2011). Mechanisms of lipid  
811 oxidation in food dispersions. *Trends in Food Science & Technology*, 22(1), 3-  
812 13.

813 Ye, A., Anema, S. G., & Singh, H. (2007). Behaviour of homogenized fat globules  
814 during the spray drying of whole milk. *International Dairy Journal*, 17(4),  
815 374-382.

816 Hawrysh, Z. (1990). Integrative concepts. In F. Shahidi (Ed.), *Canola and rapeseed:*  
817 *Production, chemistry, nutrition and processing technology* (pp. 99-122). New  
818 *York, USA: Springer.*

819

820

**Table 1.**

<b>Parameters</b>	<b>(%)</b>
Moisture (%)	0.21
Fat (%)	95.31
Crude protein (%)	3.65
Ash (%)	0.10
<b>Bulk density (g/ cc)</b>	0.44
<b>Lipid analysis</b>	<b>(g FA/ 100g fat)</b>
Total saturated fatty acids	15.16
C18:1 n-9 & n-7 (Oleic & other cis) acids	22.9
C18:2 n-6 cis (Linoleic acid)	49.9
C18:3 n-3 cis (Linolenic acid)	5.5

821

822

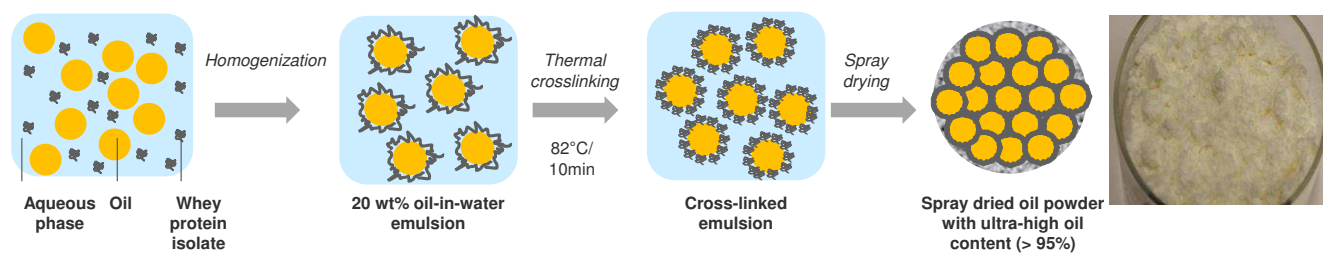
823 **Table 2.**

<b>2-Stage homogenization pressure (number of passes × bars)</b>	<b>Droplet size (d<sub>32</sub>) of initial emulsion (μm)</b>	<b>Droplet size (d<sub>32</sub>) of cross-linked emulsion (μm)</b>	<b>Particle size (d<sub>32</sub>) of spray dried emulsion (μm)</b>	<b>Oil release (wt%)</b>
<b>2 x 100/ 25</b>	2.31 ± 0.12	2.42 ± 0.36	42.88* ± 0.95	7.54** ± 0.21
<b>1 x 200/ 100</b>	0.76 ± 0.08	1.21 ± 0.21	37.27* ± 0.87	4.1** ± 0.58
<b>1 x 400/ 100</b>	0.38 ± 0.05	0.67 ± 0.04	37.73* ± 1.1	0.93** ± 0.11
<b>1 x 1200/ 100</b>	0.21 ± 0.02	0.33 ± 0.01	39.49* ± 1.26	2.73** ± 0.52

824

825

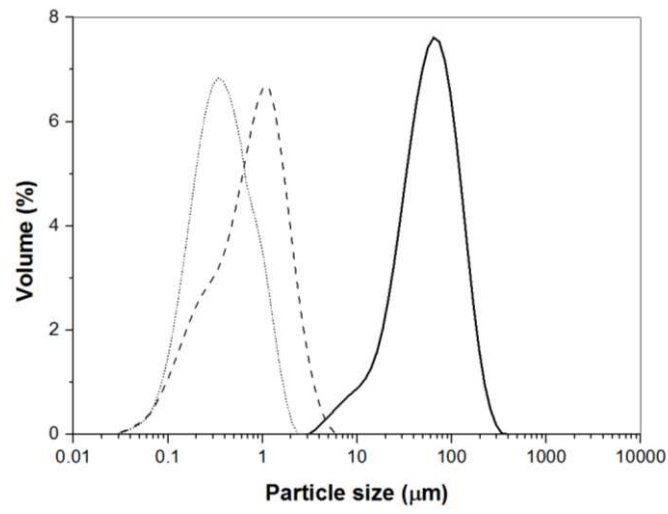
**Figure 1.**



826

827

828 **Figure 2.**



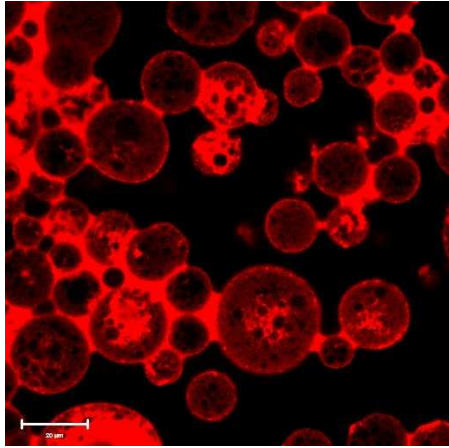
829

830

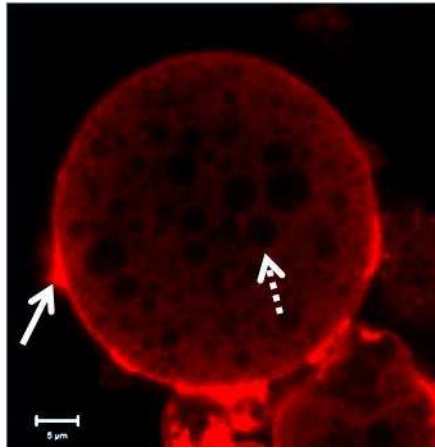
831 **Figure 3.**

832

(A)



(B)

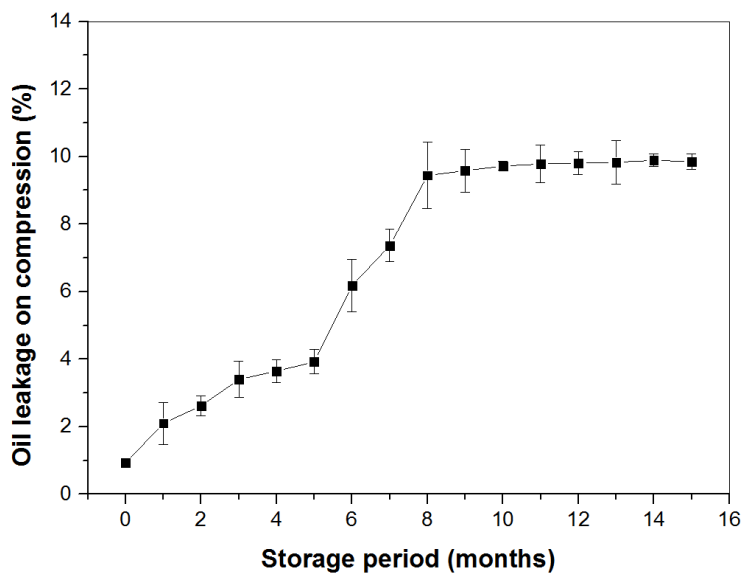


833

834

835

836 **Figure 4.**



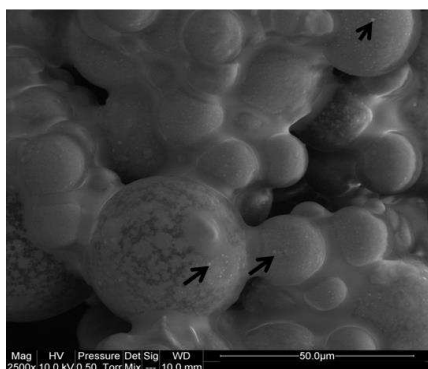
837

838

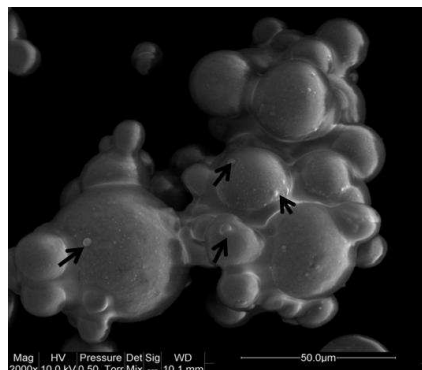
839

840 **Figure 5**

(A)



(B)



(A')



(B')

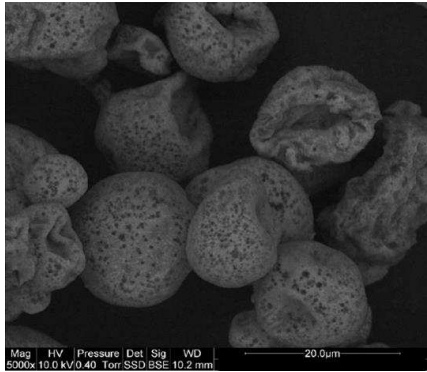


841

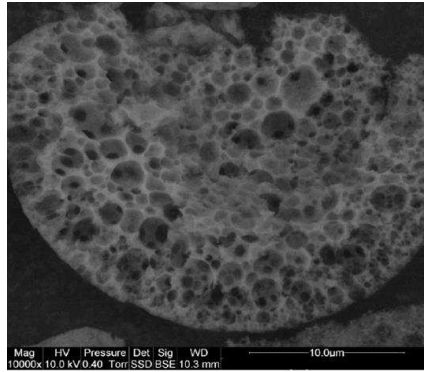
842

843 **Figure 6**

(A)



(B)

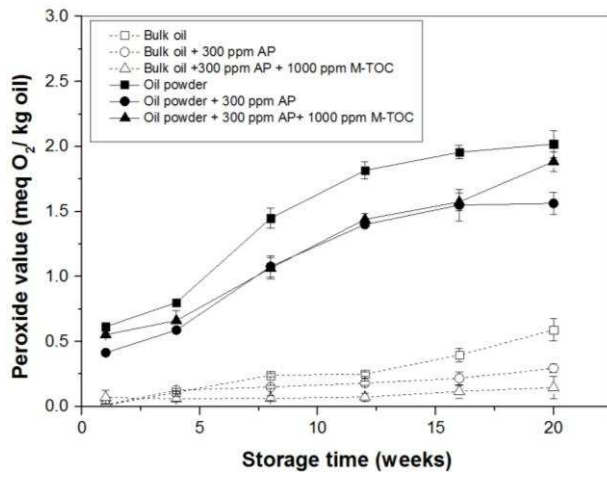


844

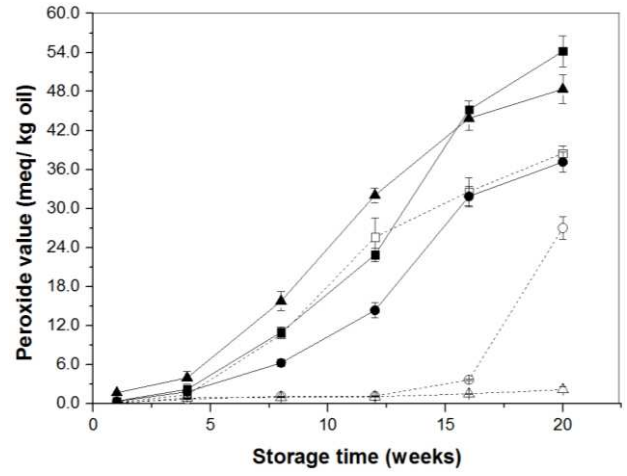
845

846 **Figure 7**

(A)

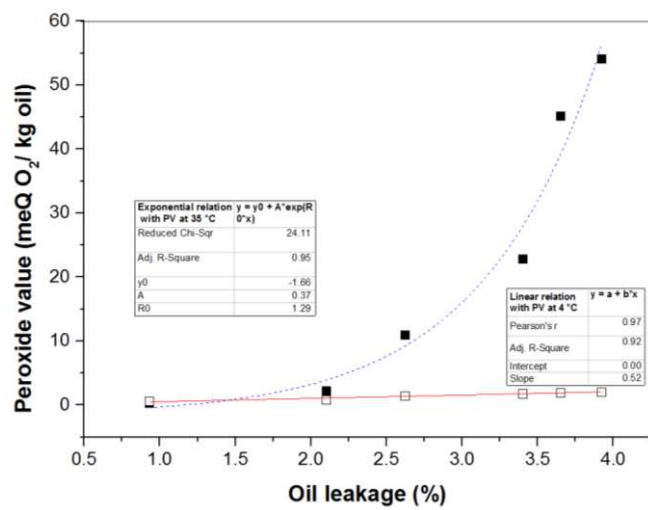


(B)



847

848 **Figure 8**

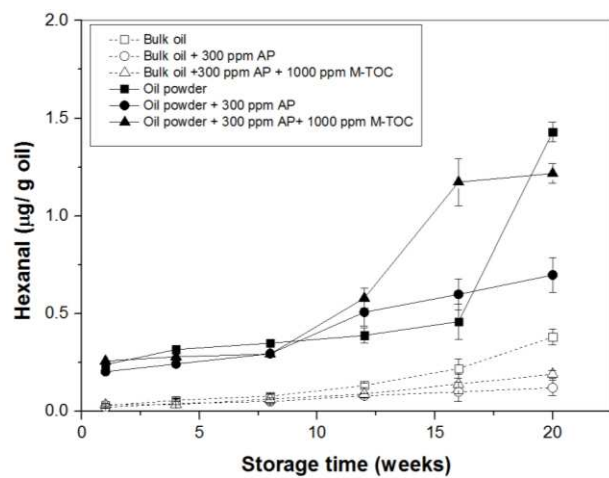


849

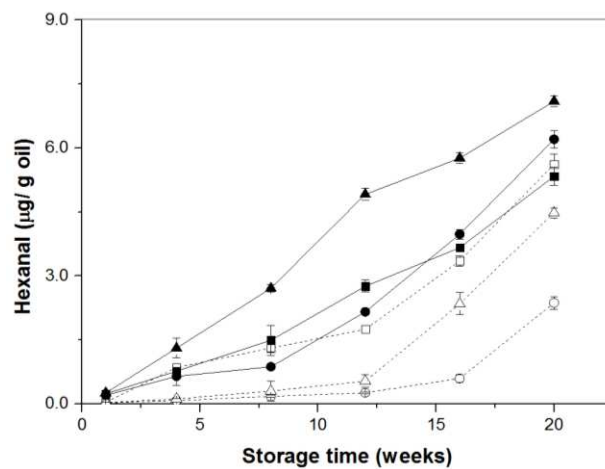
850

851 **Figure 9**

(A)



(B)



852

853

854 **Captions for Tables**

855

856 Table 1. Composition of oil powder.

857

858 Table 2. Mean particle size and oil release on compression as a function of  
859 homogenization speed of manufacturing of emulsion. Values are means of five  
860 measurements with  $\pm$  standard deviation. \*T-test indicates significant  
861 difference ( $p < 0.05$ ) when compared to  $d_{32}$  values of both emulsions with and  
862 without crosslinking; \*\* indicates significance of linear correlation of oil  
863 release (%) to droplet size,  $p < 0.05$ .

864

865           **Captions for Figures**

866

867           Figure 1. Schematic illustrations of steps of production of oil powder with  
868           ultra-high oil content showing the visual aspect (macrostructural image).

869

870           Figure 2. Droplet size distributions of the 20 wt% oil-in-water emulsion  
871           (dotted line), after heat treatment at 82 °C/ 10 minutes (dash line) and particle  
872           size distribution of the resulting oil powder (solid line).

873

874           Figure 3. Confocal micrograph of oil powder, scale bar represents 20 µm (A)  
875           and higher magnification image showing the internal structure of one powder  
876           granule containing the cross-linked emulsion droplets, scale bar represents 5  
877           µm (B). Colour in red represents the protein stained by Rhodamine 6G. Dotted  
878           arrow represents protein layers protecting individual oil droplets within a  
879           powder granule and solid arrow represents the protein shell of the granule.

880

881           Figure 4. Long-term mechanical stability of oil powder as a function of  
882           storage period. Mean value is the average of five measurements. Error bars  
883           represent standard deviations.

884

885           Figure 5. Scanning electron micrographs of spray-dried oil powders on (A) 0  
886           day and after storage for (B) 9 months. Corresponding internal images of the  
887           microstructures are showed by A' and B', respectively. Arrows in the  
888           micrographs indicate “free” surface oil.

889

890 Figure 6. Scanning electron micrographs of stored spray-dried oil powder after  
891 removal of “hexane extractable” surface oil. (A) External and (B) internal  
892 images of the microstructures.

893

894 Figure 7. Evolution of hydroperoxides in bulk oil and oil powders containing  
895 different antioxidants when stored at 4°C (A) and 35 °C over a period of 5  
896 months. Mean value is the average of five measurements. Error bars represent  
897 standard deviations.

898

899 Figure 8. Evolution of hydroperoxides in oil powders when stored at 4° C (□)  
900 and 35 °C (■) over a period of 5 months as a function of oil leakage. Solid and  
901 dashed line represents correlation at 4° C and 35 °C, respectively.

902

903 Figure 9. Evolution of hexanal in bulk oil and oil powders containing different  
904 antioxidants when stored at 4°C (A) and 35 °C over a period of 5 months.  
905 Mean value is the average of five measurements. Error bars represent standard  
906 deviations.

907

908